INELASTIC INTERACTION OF 660-*Mev PROTONS WITH CARBON NUCLEI*

A. P. ZHDANOV and P. I. FEDOTOV

Radium Institute, Academy of Sciences, U.S.S.R.

Submitted to JETP editor June 24, 1961

J. Exptl. Theoret. Phys. (U.S.S.R.) **41**, 1870-1878 (December, 1961)

The applicability of the Serber-Goldberger model to the calculation of intranuclear cascades in light nuclei is considered. Some properties of light nuclei that can significantly affect the calculations are discussed. The following factors are taken into account in the calculation of a cascade in a carbon nucleus: 1) collisions of nucleons with α-type substructures, 2) variation of the density of nuclear matter from the center to the periphery of a nucleus, 3) the momentum distribution of nucleons in light nuclei, and 4) processes involving meson production. Satisfactory quantitative agreement is obtained between the calculations and experiment.

EXPERIMENTAL investigations of interactions between nuclei and high-energy particles (of at least a few hundred Mev) show that these interactions can be regarded basically as a succession of collisions between an incoming particle and individual nucleons within a nucleus (the Serber-Goldberger model [1,2]). A comparison between calculations of the intranuclear cascade based on this model and experimental data indicates that the ideas of Serber and of Goldberger are very fruitful for the study of reactions in heavy nuclei ($A \gtrsim 100$). The applicability of these ideas to light nuclei such as C, N, and O is much less certain. This results from a number of specific properties of light nuclei, which we shall consider, as well as from the meagerness and unreliability of experimental data on interactions between high-energy particles and light nuclei.

Calculations that have been attempted [3,4] for light nuclei neglecting the aforementioned properties have not led to satisfactory agreement with experiment. However, it has been noted in [3,5], and especially in [6], that certain particular angular and energy distributions represent correctly the general character of the corresponding experimental distributions. The mean values of some calculated parameters also agree with experiment, thus indicating the possibility, in principle, of applying the Serber-Goldberger ideas to light nuclei.

THE NUCLEAR MODEL

For a more complete understanding of the degree to which the ideas of Serber and Goldberger can be used to calculate the intranuclear cascade in light nuclei a detailed quantitative comparison of the theory and experiment is required. For this purpose we need much reliable experimental data and some modification of the Serber-Goldberger model to take into account more recent information regarding the mechanism of nuclear interactions. The most typical characteristics of inelastic interactions between high-energy particles and light nuclei, differing from similar interactions with heavy nuclei, are the following.

1. The analysis of experimental information regarding the spallation of light nuclei shows that in addition to nucleons more complex structures, mainly α particles, participate in the intranuclear cascade. This has been confirmed by theoretical studies. The strong correlation between nucleons in real nuclei, according to the Brueckner model, [7,8] should result in the formation of a quasi-stable cluster of several nucleons. It is shown in [9-11] that the formation of α groups is most probable. The considerable experimental fraction ($\sim 20\%$) of cascade α particles indicates that α groups must be taken into account in the intranuclear cascade calculation. Details of the calculation of the given collisions will be presented below.

2. In an investigation of 96-Mev proton scattering on carbon and sulfur at 40° Strauch and Titus [12] detected a number of proton energy peaks, which they associate with the excitation of C_6^{12} and S_{16}^{32} levels. Several similar investigations at different proton energies were subsequently published. According to the shell model the peaks result from the excitation of single-particle and, to some extent, collective levels in the given nuclei.

Under our experimental conditions we are interested in the integral cross sections for the ex-

citation of levels above 10 Mev, because at lower excitations U carbon spallation cannot be observed in a nuclear emulsion. The estimated cross section (for U > 10 Mev) does not exceed 1% of the total inelastic scattering cross section. Resonance can therefore be neglected in calculating an intranuclear cascade.

3. Experimental scattering of high-energy electrons on different nuclei has shown that the concept of the nucleus as a sphere with a sharply defined boundary and with uniform density of nuclear matter is unrealistic even for heavy nuclei. These experiments have furnished two parameters characterizing the distribution of nuclear charge, and therefore the distribution of nuclear matter, in light nuclei. These parameters are the radius of an approximately uniform charge distribution within the nucleus and the thickness of the surface layer in which the charge density decreases smoothly. Light nuclei do not appear to contain a central region of uniform density. Therefore, if quantitative comparisons between calculations and experiment are to be made, a nuclear model with nonuniform density is required at least in the case of light nuclei.

Detailed studies of the charge density distribution in C_6^{12} have been presented in [13-15]. Good agreement is obtained between the data on high-energy electron scattering by carbon and the charge density distribution

$$\rho(r) = \rho_0 (1 + \alpha r^2/a_0^2)\, e^{-r^2/a_0^2}, \qquad (1)$$

where $\alpha = 4/3$, and the parameter a_0 is proportional to the rms radius. The best agreement with experiment is obtained at $a_0 = 1.64 \times 10^{-13}$ cm.

When the calculation of the intranuclear cascade is based on a nuclear model with varying density the determination of the nucleon mean free path in the nucleus is complicated considerably. Since the latter calculation is being performed for the first time, we shall first discuss certain factors affecting the determination of the nucleon mean free path within the nucleus.

The "random selection" of the nucleon mean free path in a nucleus is performed using the function

$$F(Y') = 1 - e^{-Y'}, \qquad Y' = \sigma(E) \int_0^x \rho(x')\, dx',$$

where $\rho(x)$ is the nucleon density at the point x, and $\sigma(E)$ is the total nucleon-nucleon interaction cross section. Using the known form of $\rho(r)$, we plot curves $Y_r(x) = \int_0^x \rho(x')\, dx'$ for different values of the impact parameter r_i. When $\rho(r)$ is given by (1), we obtain

$$Y_r(x) = \{(K_1 + K_2')\,\Phi(t') - K_3 t' e^{-t'^2/2}\}\Big|_0^{\frac{\sqrt{2}}{2}\sqrt{R^2 - r_i^2}}$$

$$- \{(K_1 + K_2')\,\Phi(t') - K_3 t' e^{-t'^2/2}\}\Big|_0^{\sqrt{R^2 - r_i^2} - \frac{a_0}{\sqrt{2}} t'},$$

$$t'(x) = \frac{\sqrt{2}}{a_0}\left(\sqrt{R^2 - r_i^2} - x\right),$$

$$K_1 = \frac{\sqrt{\pi}}{2} \rho_0 a_0 e^{-(r_i/a_0)^2}\left(1 + \alpha \frac{r_i^2}{a_0^2}\right),$$

$$K_2' = \frac{\sqrt{\pi}}{2} \rho_0 a_0 \alpha e^{-(r_i/a_0)^2}, \qquad K_3 = \frac{1}{\sqrt{2}} \rho_0 a_0 \alpha e^{-(r_i/a_0)^2},$$

where $\Phi(t')$ is the probability integral. The value $\rho_0 = 0.18$ nucleon/$(10^{-13}\text{cm})^3$ is obtained from the relation

$$4\pi\rho_0 \int_0^\infty \left(1 + \alpha \frac{r^2}{a_0^2}\right) e^{-(r/a_0)}\, r^2 dr = A.$$

Figure 1 shows the $Y_r(x)$ curves for several different values of the impact parameter r_i.

From a table of random numbers and functions $F(Y')$ we pick some number Y' and obtain $Y'/\sigma(E) = Y$. The nucleon mean free path in the nucleus is then determined from the curve corresponding to a specific value of r_i.

Although the Fermi gas model for T = 0 has been used quite successfully, the neglect of intranuclear interactions between nucleons must be regarded as a limiting assumption. In actuality, the existence of such processes as capture or the ejection of nucleon groups indicates that interactions between nucleons occur. This means that the momentum distribution of intranuclear nucleons differs from the Fermi distribution for T = 0. Therefore a Fermi gas model for $T \neq 0$ will be a more realistic nuclear model. Information regarding the momentum distribution of nucleons in the nuclear ground state can be obtained from the angular and energy distributions of nuclear interaction products produced by high-energy particles. From investigations of the quasi-elastic scattering of fast protons in light nuclei [16-18] it has been found that the energy spectra of scattered protons agree with a Gaussian momentum distribution of nucleons in Be, C, and O nuclei, with the 1/e value occurring at 13—20 Mev.

For our calculation we used the distribution obtained by the Meshcheryakov group, [17] who had studied the angular and energy distributions of

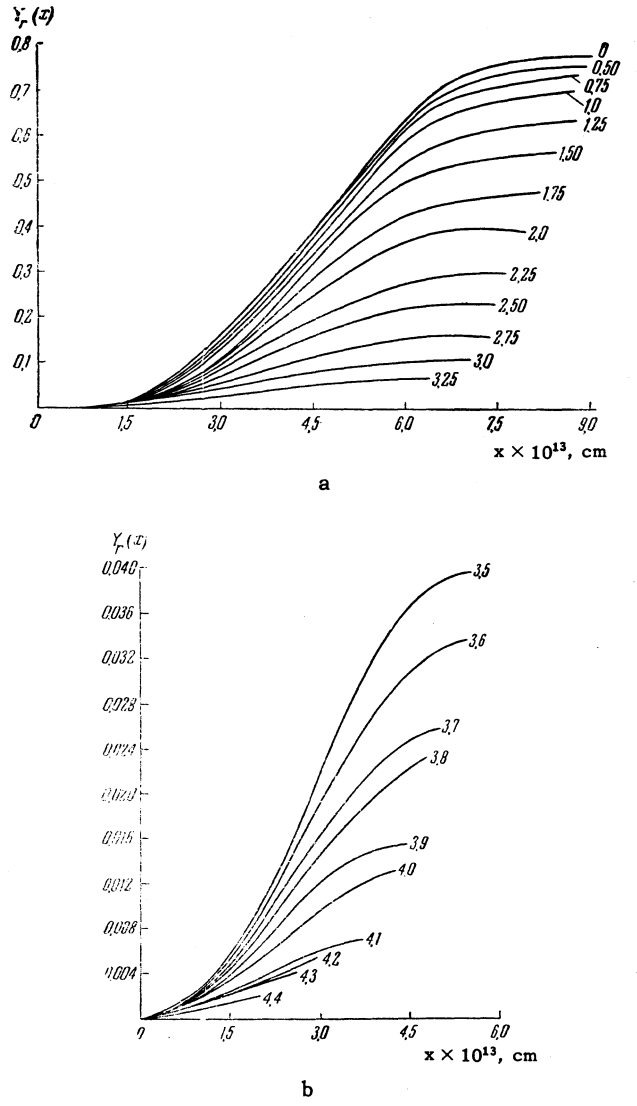

FIG. 1. $Y_r(x)$ curves used in determining the nucleon mean free path in the nucleus. Each curve is labeled with the corresponding impact parameter.

secondary protons from p-Be, p-C, p-Cu, and p-U collisions at 660 Mev. The data for Be and C indicate a Gaussian distribution of nucleon momentum with the 1/e value at 20 Mev.

In calculating the intranuclear cascade we also took into account the production, absorption, and scattering of pions on nucleons. For meson production we used the model whereby pions are produced only through an excited $p_{3/2,3/2}$ nucleon resonance state. Satisfactory agreement with experiment was not obtained from a simpler model of pion production. [19]

COMPARISON OF CALCULATIONS AND EXPERIMENT. DISCUSSION

The computed results presented in this section are based on 500 calculated interactions between 660-Mev protons and C_6^{12} nuclei. The intranuclear cascades were calculated by the Monte Carlo method for relativistic three-dimension kinematics with uniform (ρ = const) and varying ($\rho \neq$ const) density of nuclear matter in C_6^{12}.

In order to investigate the aforementioned interaction experimentally we introduced a suspension of diamond dust into a nuclear emulsion registering particles with minimum ionization. The transparency of the diamond particles permits selection of the requisite spallations and guarantees high reliability of the data. We have described this technique in greater detail in [20,21], where we reported results for the low-energy spallation products of C_6^{12}.

a) Absorption cross section. In computing the radius of the C_6^{12} nucleus to be used in our cascade calculations we took $r_0 = 1.36 \times 10^{-13}$ cm. This value of r_0 for the equivalent uniform model of the carbon nucleus was obtained from experiments on charge density distribution in C_6^{12}. The total and diffraction cross sections calculated from the optical model for the interaction between 650-Mev protons and C_6^{12} are in best agreement with experiment for $r_0 = 1.37 \times 10^{-13}$ cm, [22] which practically coincides with our value for r_0.

We computed the following absorption cross sections: σ_a = 220 mb for a nucleus with uniform density, and σ_a = 235 mb for a nucleus with varying density of nuclear matter. We cannot compare these results with a corresponding experimental value from our own work. An experimental cross section cannot be computed with sufficient accuracy for the purpose of comparison, since we did not know the exact magnitude of the proton flux irradiating the nuclear emulsions. However, we can compare our calculations with the experimental results obtained by other investigators under more or less similar conditions. The most suitable data for this purpose are the cross sections for interactions between 650-Mev protons and different nuclei, given in [22]. The cross section σ_a = 227 ± 12 mb for carbon is in very good agreement with our calculation. The absence of any appreciable difference between the calculated absorption cross sections for ρ = const and $\rho \neq$ const is due to the equivalence of both models for the interaction cross section. This determined the selection of r_0 in computing the radius of a uniformly dense carbon nucleus.

b) Cross sections for quasi-elastic p-p and n-p interactions. One of the most serious discrepancies between the calculations and experiment occurred in the case of the cross sections for quasi-elastic nucleon-nucleon scattering. The

experimental cross sections were two to three times larger than the computed cross sections for both heavy and light nuclei. Quasi-elastic proton scattering on carbon has been studied with 660- and 930-Mev protons.[17,18] At 930 Mev[18] the quasi-elastic p-p scattering cross section $\sigma^{q.e.}$ was 46 ± 10 mb. Cross sections of 95—100 mb for combined quasi-elastic p-p and p-n scattering are obtained by angular integration of the proton energy spectra in [17]. When this combined cross section is compared with the ratio σ_{pp}/σ_{np} for elastic scattering on free nucleons we find that at 660 Mev $\sigma_{pp}^{q.e.} \approx 46$ mb and $\sigma_{pn}^{q.e.} \approx 54$ mb. It is suggested in [17] that the disagreement between the computed and experimental cross sections for quasi-elastic scattering is due to failure to take diffuseness of the peripheral region of the nucleus into account in the calculation. This hypothesis is confirmed by our calculations for uniform and non-uniform nuclear density.

Table I shows that considerably improved agreement between the computed and experimental quasi-elastic scattering cross sections results when the nuclear model with varying density is used.

c) Energy and angular distributions of cascade protons. Table II compares the average numbers of cascade protons ($\bar{n}_p$), neutrons ($\bar{n}_n$), and nucleons ($\bar{n}_N$), and the average number of collisions per spallation ($\bar{n}$) derived from both the calculations and experiments.

Since in most instances we cannot determine whether a given emulsion track is produced by a proton or a meson, charged pions are included in the computed value of $\bar{n}_p$ for the purpose of comparison with experiment. The total values including pions are given in parentheses. The fairly high average number of collisions per cascade

Table I

Cross section	$\sigma_{pp}^{q.e.}$, mb	$\sigma_{pn}^{q.e.}$, mb
Experiment	46±10	54±12
Computation (ρ = const)	17±3	19±3
Computation ($\rho \neq$ const)	33±5	33±5

Table II

	$\bar{n}_p$	$\bar{n}_n$	$\bar{n}_N$	$\bar{n}$
Computation (ρ = const)	2.17 (2.56)	1.20	3.37	2.70
Computation ($\rho \neq$ const)	1.87 (2.18)	1.00	2.87	2.20
Experiment	(2.00)	—	—	—

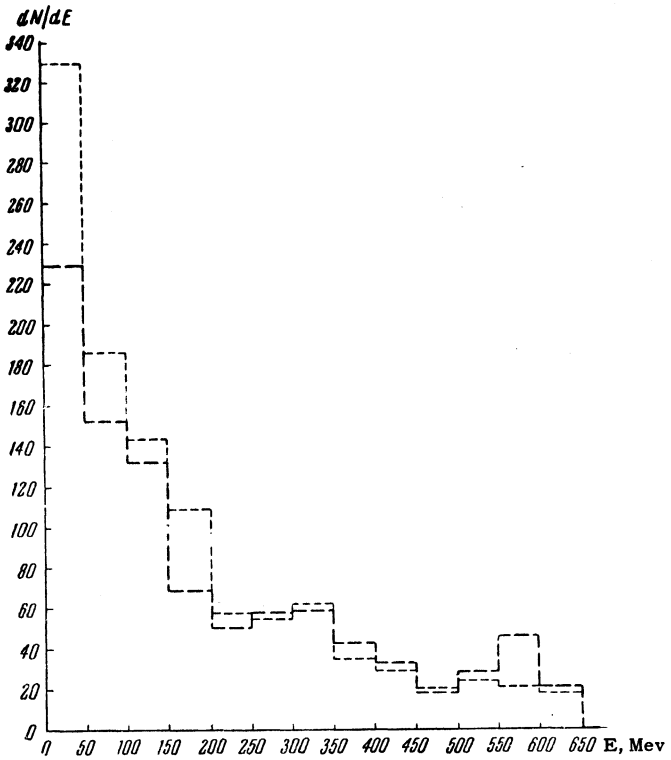

FIG. 2. Computed energy distribution of cascade protons (all U). Long dashes – for $\rho \neq$ const; short dashes – for ρ = const.

even for $\rho \neq$ const results to a considerable extent from the contribution made by pion collisions with intranuclear nucleons. A 100—200 Mev meson has a short mean free path in nuclear matter and sometimes undergoes elastic scattering or scattering with charge transfer before being absorbed or escaping from the nucleus.

Figures 2 and 3 show the computed energy and angular distributions of cascade protons of all energies. It was shown in [17] that the energy spectra of protons from different bombarded nuclei including carbon exhibit a pronounced peak at high energies, corresponding to quasi-elastic single proton-nucleon collisions. The computed spectrum for $\rho \neq$ const in Fig. 2 also has a peak at 500—600 Mev, whereas for ρ = const we observe a continuous decrease of the proton count with increasing energy.

There are no essential differences between the angular distributions computed for C_6^{12} with uniform and varying densities. The angular distribution of protons for ρ = const was, as could be expected, smeared out more toward large angles than for $\rho \neq$ const, since nucleons experience a larger average number of collisions in the nucleus. In a comparison of the computed and experimental spectra the following considerations must be taken into account.

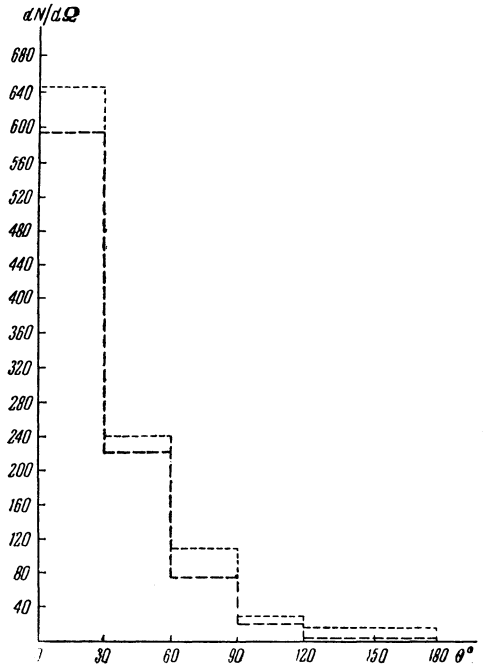

FIG. 3. Computed angular distribution of cascade protons (all U). Long dashes – for $\rho \neq$ const; short dashes – for ρ = const.

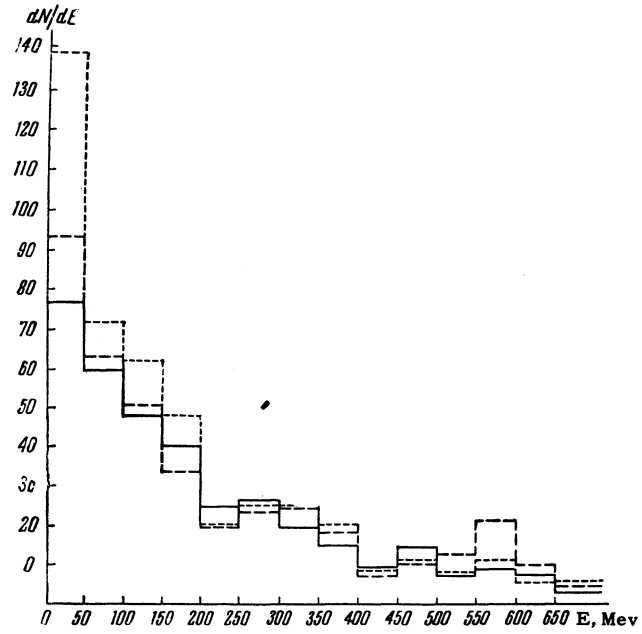

FIG. 4. Energy distribution of cascade protons. Solid line – experimental; long dashes – computed for $\rho \neq$ const; short dashes – computed for ρ = const.

1. The experimental spectra did not take into account one-prong and two-prong stars without a slow-particle track, because the registration of these stars is not sufficiently reliable. In our calculation of the spectra we therefore had to exclude interactions in which, after the emission of one or two cascade protons, the excitation energy U of the residual nucleus is insufficient for the emission of at least one proton or α particle. Our calculations showed that there are no essential differences between proton spectra including all interactions and the spectra including only interactions with $U > U_p$, where U_p is the excitation energy that would permit the residual nucleus to emit at least one proton or α particle. A small difference appears only in the enhanced average number of protons per cascade, due mainly to a larger number of cascade protons in the low-energy portion of the spectrum.

2. The computed spectra had to include charged pions, since singly charged particles were not divided experimentally into protons and pions. Each pion in the computed energy spectra was replaced by a proton having the energy for which the proton would induce the same ionization in the emulsion as the corresponding pion.

In Figs. 4 and 5 the angular and energy spectra computed with the foregoing considerations taken into account are compared with the corresponding experimental distributions. Figure 4 shows that the total experimental number of cascade protons and the overall shape of the experimental spectrum agree satisfactorily with the calculations for $\rho \neq$ const. The discrepancy at high energies is due to insufficient resolution when determining proton energies in this region. The experimental angular distribution of cascade protons is also in better agreement with the calculation for $\rho \neq$ const.

The foregoing comparison of the computed and experimental results shows that the improvements of the nuclear model for the study of the intranuclear cascade in light nuclei lead to satisfactory

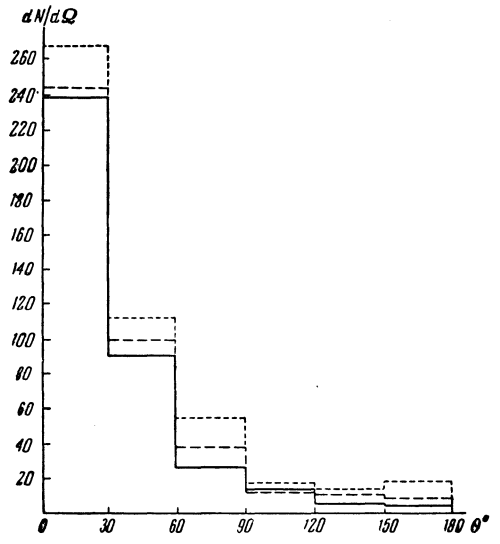

FIG. 5. Angular distribution of cascade protons. Solid line – experimental; long dashes – computed for $\rho \neq$ const; short dashes – computed for ρ = const.

quantitative agreement with experiment. Further confirmation is found in a comparison of the computed and experimental yields of residual nuclei and in the excitation-energy distributions determined by analyzing carbon spallations. A discussion of the pertinent data will be published separately.

The authors wish to thank V. V. Chavchanidze for valuable suggestions regarding the calculating procedure, G. M. Subbotina for assistance with the calculations, L. I. Shur and I. V. Ryzhkova for preparation of the emulsions, and V. N. Kuz'min and I. M. Kuks for useful discussions.

[1] R. Serber, Phys. Rev. **72**, 1114 (1947).

[2] M. Goldberger, Phys. Rev. **74**, 1269 (1948).

[3] J. Combe, Nuovo cimento Supplemento **3**, 182 (1956).

[4] H. Muirhead and W. G. V. Rosser, Phil. Mag. **46**, 652 (1955).

[5] A. P. Zhdanov and F. G. Lepekhin, Trudy Radievogo instituta AN SSSR (Trans. Radium Institute) **9**, 41 (1959).

[6] Petrov, Ivanov, and Rusakov, JETP **37**, 957 (1959), Soviet Phys. JETP **10**, 682 (1960).

[7] Brueckner, Eden, and Francis, Phys. Rev. **98**, 1445 (1955).

[8] H. A. Bethe, Phys. Rev. **103**, 1353 (1956).

[9] A. I. Baz', JETP **31**, 831 (1956), Soviet Phys. JETP **4**, 704 (1957).

[10] M. Rotenberg and L. Wilets, Phys. Rev. **110**, 1126 (1958).

[11] V. G. Solov'ev, DAN SSSR **131**, 286 (1960), Soviet Phys.-Doklady **5**, 298 (1960).

[12] K. Strauch and W. F. Titus, Phys. Rev. **95**, 854 (1954).

[13] J. H. Fregeau and R. Hofstadter, Phys. Rev. **99**, 1503 (1955).

[14] J. H. Fregeau, Phys. Rev. **104**, 225 (1956).

[15] Ehrenberg, Hofstadter, Meyer-Berkhout, Ravenhall, and Sobottka, Phys. Rev. **113**, 666 (1959).

[16] Cladis, Hess, and Moyer, Phys. Rev. **87**, 425 (1952).

[17] Azhgireĭ, Vzorov, Zrelov, Meshcheryakov, Neganov, Ryndin, and Shabudin, JETP **36**, 1631 (1959), Soviet Phys. JETP **9**, 1163 (1959).

[18] Dowell, Frisken, Martelli, and Musgrave, Proc. Phil. Soc. (London) **75**, 24 (1960).

[19] Metropolis, Bivins, Storm, Miller, Friedlander, and Turkevich, Phys. Rev. **110**, 204 (1958).

[20] A. P. Zhdanov and P. I. Fedotov, Pribory i tekhnika éksperimenta (Instruments and Experimental Techniques) No. 3, 133 (1959).

[21] A. P. Zhdanov and P. I. Fedotov, JETP **37**, 392 (1959), Soviet Phys. JETP **10**, 280 (1960).

[22] V. I. Moskalev and B. V. Gavrilovskii, DAN SSSR **110**, 972 (1956), Soviet Phys.-Doklady **1**, 607 (1956).

Translated by I. Emin
318